

# Promotion of the transdermal delivery of protein drugs by *N*-trimethyl chitosan nanoparticles combined with polypropylene electret

Ye Tu<sup>1,2,\*</sup>  
 Xinxia Wang<sup>3,\*</sup>  
 Ying Lu<sup>2,\*</sup>  
 He Zhang<sup>2</sup>  
 Yuan Yu<sup>2</sup>  
 Yan Chen<sup>2</sup>  
 Junjie Liu<sup>2</sup>  
 Zhiguo Sun<sup>2</sup>  
 Lili Cui<sup>4</sup>  
 Jing Gao<sup>2</sup>  
 Yanqiang Zhong<sup>2</sup>

<sup>1</sup>Department of Medical Affairs, East Hospital, Tongji University School of Medicine, <sup>2</sup>Department of Pharmaceutical Science, School of Pharmacy, Second Military Medical University, <sup>3</sup>Department of Pharmacy, East Hospital of Hepatobiliary Surgery, <sup>4</sup>Department of Inorganic Chemistry, School of Pharmacy, Second Military Medical University, Shanghai, People's Republic of China

\*These authors contributed equally to this work

**Abstract:** We recently reported that electret, which was prepared by a corona charging system with polypropylene film, could enhance the transdermal delivery of several drugs of low molecular weight. The aim of this study was to investigate whether electret could enhance the transdermal delivery of protein drugs by *N*-trimethyl chitosan nanoparticles (TMC NPs) prepared by an ionic gelation method. A series of experiments were performed, including in vitro skin permeation assays and anti-inflammatory effects, to evaluate the transdermal delivery of protein drugs by TMC NPs in the presence of electret. The results showed that in the presence of electret, the transdermal delivery of protein drugs in TMC NPs was significantly enhanced, as demonstrated by in vitro permeation studies and confocal laser scanning microscopy. Notably, superoxide dismutase-loaded TMC NPs combined with electret exhibited the best inhibitory effect on the edema of the mouse ear. TMC NPs combined with electret represent a novel platform for the transdermal delivery of protein drugs.

**Keywords:** *N*-trimethyl chitosan nanoparticles, electret, transdermal delivery, protein drugs

## Introduction

Recently, numerous studies have been performed on the transdermal drug delivery of protein drugs. Compared with other administration routes, transdermal drug delivery has many advantages such as improved bioavailability and increased patient compliance.<sup>1</sup> However, transdermal delivery of protein drugs is severely hampered by the stratum corneum (SC), a main barrier for transdermal delivery.<sup>2</sup> Only a minority of lipophilic molecules could effectively penetrate SC.<sup>3</sup> A variety of approaches have been developed to promote the transdermal delivery of drugs. These approaches include chemical enhancers,<sup>4,5</sup> iontophoresis,<sup>6,7</sup> electroporation,<sup>8</sup> microneedles,<sup>9,10</sup> sonophoresis<sup>11,12</sup> and laser ablation.<sup>13</sup> Although significant progress has been made in the transdermal delivery of drugs, there still exist many disadvantages such as skin irritation,<sup>14</sup> high production costs<sup>15</sup> and inconvenience.<sup>13</sup> Thus, it is urgent to develop a low-toxic, low-cost, convenient and efficient transdermal delivery system.

Electret is a dielectric material that can maintain a quasi-permanent electric charge or dipole polarization for a long time.<sup>16</sup> It can carry different surface potentials in volts and produce long-term microcurrent and electrostatic field at the skin to regulate the electret state of the skin.<sup>17</sup> Thus, the microcurrent and electrostatic field of the electret could function as a physical factor to enhance the transdermal drug delivery by regulating the arrangement and fluidity of lipid bilayers and the structure of proteins in SC, widening the gaps on the surface of the skin.<sup>18</sup> We recently reported that

Correspondence: Yanqiang Zhong;  
 Jing Gao  
 Department of Pharmaceutical Science,  
 School of Pharmacy, Second Military  
 Medical University, 325 Guohe Road,  
 Shanghai 200433, People's Republic  
 of China  
 Tel/fax +86 21 8187 1285;  
 +86 21 8187 1293  
 Email zyzsmmu@126.com;  
 gjsmmu@126.com

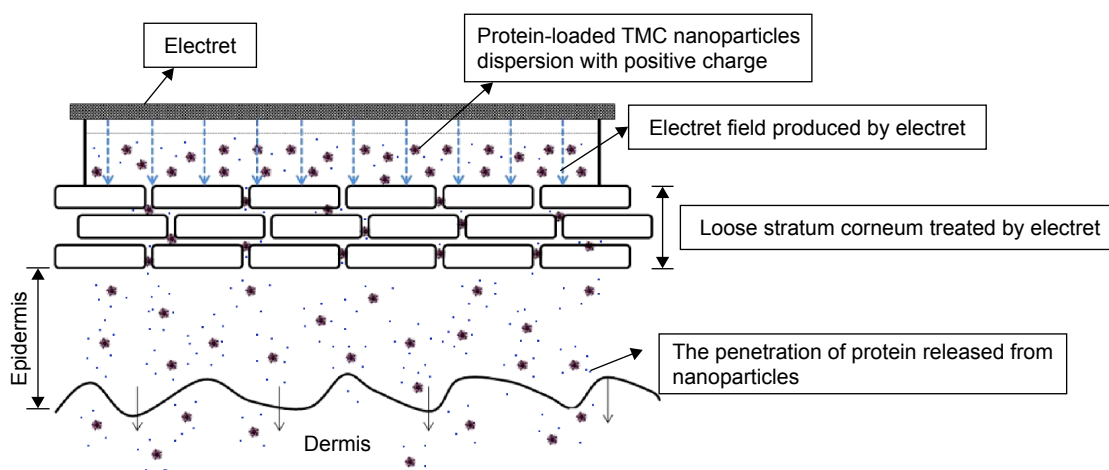


**Figure 1** The transdermal delivery system of TMC NPs combined with electret.

**Abbreviations:** TMC, *N*-trimethyl chitosan; NPs, nanoparticles.

electret could effectively enhance the transdermal delivery of several drugs of low molecular weight, such as methyl salicylate,<sup>19</sup> meloxicam,<sup>20</sup> lidocaine<sup>21</sup> and cyclosporine A (a small peptide, 1024 Da).<sup>22</sup> However, our results showed that electret could not significantly promote the transdermal delivery of protein drugs with higher molecular weights (Tu et al, unpublished data, 2011), which is consistent with the result obtained by Murthy et al<sup>23</sup> that electret could not enhance the transdermal delivery of protein drugs with high molecular weights >1 kDa.

Chitosan is a mucoadhesive and positively charged polysaccharide and could improve the transdermal delivery of several drugs.<sup>24,25</sup> Recently, several studies have showed improved transdermal delivery of drugs by nanoparticles (NPs) composed of chitosan and other polymers such as poly(lactide-co-glycolide) and pluronic.<sup>1,2</sup> *N*-trimethyl chitosan (TMC) is the most frequently studied chitosan, due to its well-defined structures, improved solubility and easy preparation.<sup>26</sup> Many studies have shown that TMC NPs could significantly enhance the drug absorption across mucosa epithelia.<sup>27–30</sup> TMC NPs have been shown to increase the immunogenicity of subunit antigens after nasal administration.<sup>31</sup> Similarly, TMC NPs could also significantly enhance the transdermal delivery of drugs.<sup>32</sup> The proposed mechanisms by which chitosan and its derivatives promote the transdermal delivery of drugs are that they can loosen the compact structure of keratin in SC, widen the tight junctions in the skin or interact with negatively charged SC cells.<sup>1,26</sup> It is noteworthy that TMC NPs are an effective positively charged transdermal delivery system; therefore, we hypothesize that TMC NPs may exert enhanced transdermal delivery of protein drugs in the presence of electret.

In this study, to enhance the transdermal delivery of protein drugs, we have developed TMC NPs loaded with proteins, using an ionic gelation method. The NPs were further investigated for *in vitro* skin permeation assays and anti-inflammatory effects in the absence or presence of electret, which was prepared by a corona charging system with polypropylene (PP) film (Figure 1).

## Materials and methods

### Materials

Chitosan of low molecular weight with a deacetylation degree of 75%–85%, ammonium persulfate (APS), fluorescein isothiocyanate (FITC), [2-(methacryloyloxy)ethyl]trimethylammonium chloride (TMAEMC) and bovine serum albumin (BSA) were purchased from Sigma (St Louis, MO, USA). Sodium tripolyphosphate (TPP) was obtained from Fluka, USA. Superoxide dismutase (SOD, 30 kDa) was purchased from Amresco (Solon, OH, USA). The enzyme-linked immunosorbent assay (ELISA) kit for quantitative analysis of SOD was provided by Shanghai Jingma Biotechnology Co. Ltd, Shanghai, China. Indomethacin was purchased from Shanghai Yifeng Pharmacy (Shanghai, China). Xylene was purchased from Sinopharm Chemical Reagent Co. Ltd, Shanghai, China. PP films were bought from Toray Industry (Tokyo, Japan). All the other reagents were of analytical grade.

All Sprague Dawley (SD) rats (male, 200–250 g, ~8 weeks) and BALB/c mice (male, 20–25 g, 4–6 weeks) were purchased from the Shanghai Experimental Animal Center of Chinese Academy of Sciences (Shanghai, China). All rats and mice were placed in a pathogen-free environment and allowed to acclimate for a week before being used in studies. Our study was approved by the Committee on Animal Use of Second Military Medical University (Shanghai, China),

and all the procedures were performed in accordance with the Guidelines of the Committee on Animal Use of Second Military Medical University.

## Methods

### Preparation of FITC-labeled BSA (FITC-BSA)

FITC-BSA was prepared by the procedure described by Hentz et al.<sup>33</sup> with some modifications. Briefly, FITC was dissolved in dimethyl sulfoxide (DMSO) solution at a concentration of 8 mg/500  $\mu$ L. Then, FITC solution was added dropwise to a BSA solution dissolved in 100 mM carbonate buffer (10 mg/mL, pH 9.0). The mixture was allowed to react at room temperature overnight with gentle stirring under dark conditions. The final solution was dialyzed against deionized water using the dialysis membrane (MWCO: 12 kDa; Beijing Biodee Biotechnology Co. Ltd, Beijing, China) to remove free FITC. Finally, the FITC-BSA was lyophilized for 16–18 hours (h) using VirTis® Advantage™ Benchtop Freezer to obtain a fine powder of FITC-BSA.

### Preparation of electret

PP films with a thickness of 25  $\mu$ m and an area of 5 $\times$ 6 cm were charged at a constant voltage and 65% humidity for 10 minutes (min) using a corona charging system (Dalian University of Technology, Dalian, China). The point voltages used were  $\pm$ 10 kV, and the grid voltages were  $\pm$ 500,  $\pm$ 1,000 and  $\pm$ 2,000 V accordingly. The effective surface potentials of the charged film (electret) were measured with a surface potentiometer (ESR102A; Beijing Huajinghui Technology Co. Ltd, Beijing, China).

### Synthesis and characterization of TMC

TMC was synthesized as reported with some modifications.<sup>34</sup> Briefly, chitosan (1% w/v) was dissolved in 250 mL of 1% acetic acid solution. APS (0.045% w/v) and TMAEMC were added, and the mixture was stirred at 60°C under a nitrogen stream. The molar ratio of  $-NH_2$  of chitosan and TMAEMC was 2:1. The reaction was terminated after 4 h, and the copolymer solution was dialyzed against deionized water for 48 h and then lyophilized.

The TMC was characterized by  $^1H$  NMR. The samples were measured in  $D_2O$ , using a DMX-500 spectrometer (500 MHz; Bruker, Germany). The degree of quaternization (DQ) was calculated using the following equation 1:<sup>35</sup>

$$DQ = [(\int TM / \int H) \times (1/9)] \times 100\% \quad (1)$$

where  $\int TM$  is the integral of the trimethyl amino group (quaternary amino) peak at 3.3 ppm and  $\int H$  is the integral of the H peaks from 5.0 to 6.0 ppm.

### Preparation of TMC NPs

TMC NPs were prepared by an ionic gelation process as reported by Zhu et al.<sup>36</sup> Briefly, TMC NPs were prepared by a simple mixing procedure where an equal volume of TPP aqueous solution (1 mg/mL) was added to a TMC solution (10 mg/mL) with subsequent stirring at room temperature.

For FITC-BSA-loaded TMC NPs (FITC-BSA TMC NPs), a BSA solution (0.1 mL, 4 mg/100  $\mu$ L) was mixed with a TMC solution (0.5 mL, 10 mg/mL) under stirring. Then, a TPP aqueous solution (0.5 mL, 1 mg/mL) was added dropwise to the resultant mixture under stirring for 30 min. SOD-loaded TMC NPs (SOD TMC NPs) were prepared in the same way as FITC-BSA TMC NPs except that the SOD concentration was 2 mg/100  $\mu$ L.

To examine the penetration of TMC NPs, TMC was labeled with FITC as described later. Briefly, FITC (1 mg/mL in DMSO) was added to a TMC solution (10 mg/mL in acetate buffer, pH =4.6), and the solution was stirred for 12 h at room temperature. After dialysis against deionized water for 48 h, the resultant product was lyophilized. All procedures were carried out in the dark.

### Characterization of TMC NPs

#### Particle size and zeta potential

After the NPs were dispersed in deionized water, their size and zeta potential were analyzed using Zeta sizer Nano S (Malvern Instruments, Malvern, UK).

#### Transmission electron microscopy (TEM)

The morphological examination of the NPs was performed by TEM. Briefly, samples were prepared by dropping one drop of the NPs dispersion onto a copper grid coated with a carbon membrane. Then, the samples were stained by 2% phosphotungstic acid and dried. The NPs were visualized under the TEM (TecnaiG2 spirit Biotwin; FEI, USA).

#### Determination of the encapsulation efficacy (EE)

The EE of the NPs was determined using BSA- or SOD-loaded TMC NPs. Briefly, the unencapsulated BSA or SOD was removed by centrifugation of the NPs at 12,000 rpm at 4°C for 30 min. The supernatant containing BSA or SOD was determined by reversed-phase high-performance liquid chromatography (HPLC) or micro BCA Kit (Pierce).<sup>37</sup> The EE was calculated using the following equation 2:

$$EE = (A - B) / A \times 100\% \quad (2)$$

$A$  is the total amount of proteins, and  $B$  is the amount of free proteins in the supernatant.

The quantitative analysis of BSA or SOD was performed as described later. For the analysis of BSA, an HPLC system (Shimadzu Corp, Japan) equipped with a C18 column (Welch Materials, 5  $\mu\text{m}$ , 4.6 mm ID  $\times$  25 cm) was used. The mobile phase was 0.1% v/v trifluoroacetic acid (TFA) in water (solvent A) and 0.1% v/v TFA in acetonitrile (solvent B) and was run at a gradient of 25:75 to 60:40 (solvent A:B) from 0 to 15 min, then 25:75 (solvent A:B) from 15.01 to 23 min, respectively, with a flow rate of 1.0 mL/min. The detection wavelength was set at 280 nm. The SOD was determined by a micro BCA kit (Pierce) according to the manufacturer's protocol.

### In vitro skin permeation assays

The rats were anesthetized by intraperitoneal (i.p.) injection of pentobarbital sodium (30 mg/kg), and the hair from the abdominal region was carefully shaved using an animal hair clipper 24 h before the assays. After the rats were sacrificed, the shaved region was incised to obtain the skin. The subcutaneous fat and other visceral tissue under the skin should be removed. The skins were washed and examined for the integrity.

The incised skins were cut to appropriate size and immediately mounted in the vertical Franz-type diffusion cell (Huanghai Medicine & Drug Testing Instruments Co., Ltd, Shanghai, China). As a receptor phase, a phosphate buffered saline (PBS) buffer (pH 7.4) was filled in the receptor compartment and maintained at 37°C, under a centrifugation rate of 600 rpm. A variety of drugs were directly added to the donor side. When combined with the use of PP electrets, different corona charged PP electrets were placed ~1 mm above the surface of the drug solution. At specified time points up to 24 h, 0.4 mL of the receptor solution was withdrawn, and the receptor compartment was supplemented with the same amount of fresh PBS to maintain the total volume. The amount of permeated FITC-BSA was measured using a spectrofluorophotometer (F-7000; Hitachi, Japan) at the excitation wavelength of 496 nm and the emission wavelength of 520 nm, respectively, while permeated SOD was measured by ELISA kit (Shanghai Jing Ma Biological Technology Co., Ltd) according to the manufacturer's protocol. To evaluate the amount of protein in the skin, the protein was extracted from the skin as described previously.<sup>1</sup> Finally, the amount of the extracted protein drugs was analyzed by spectrofluorophotometry or ELISA.

To identify the skin permeation of TMC NPs, FITC-labeled TMC NPs were used. The skin permeation and

extraction assays of FITC-TMC NPs were performed in a similar way as described earlier.

### Confocal studies

A confocal study was performed to directly observe the distribution of FITC-BSA or TMC NPs in the skin after each permeation assay. Briefly, 24 h after the drug was added to the skin in the permeation assay, the diffusion area of the skin was fixed with 4% formalin solution and embedded in optimal cutting temperature compound. After that, the embedded skin was frozen in liquid nitrogen and cut into 20  $\mu\text{m}$  sections. The skin sections were visualized by a confocal laser scanning microscope (TCS-SP5; Leica, Germany). The green fluorescence of FITC was analyzed.

### Histological examinations

The histological examinations of the skin when treated by +2,000 V electret for different periods of time (4, 8 and 12 h) were performed as described later. Briefly, SD rats were anesthetized by an i.p. injection of urethane (20.0% aqueous solution, 5.0 mL/kg). Electret with the corona voltage of +2,000 V was placed on the abdomen surface of which the hair was removed 24 h before. The electret was removed 4, 8 and 12 h after its placement, and the treated skin was excised, fixed by 4% formalin, dehydrated, embedded in paraffin and cut into 8  $\mu\text{m}$  sections. Finally, the sections were stained with hematoxylin and eosin (H&E). The images were observed under a conventional light microscope (Olympus IX71 inverted microscope).

### Anti-inflammatory assays in mice

The protective role of SOD TMC NPs combined with electret on the prevention of edema induced by xylene was demonstrated in BALB/c mice. Briefly, BALB/c mice were anesthetized by an i.p. injection of urethane (20.0%, 0.5 mL/100 g). Different drugs were applied on the right ear of the mice, whereas respective vehicle or solvent (used as internal control) was applied on the left ear of the mice. At the same time, electrets were placed on the same side of the ear. After 6 h, the treated ear was challenged with 20  $\mu\text{L}$  of xylene. Half an hour later after the xylene challenge, xylene-induced edema was determined as described later. After the mice were sacrificed, the two ears were excised, cut along the auricle baseline and weighed. The edema degree of the ear was calculated by subtracting the weight of the left ear from that of the right ear. Indomethacin (90  $\mu\text{g}$  per ear), a validated anti-inflammatory drug, was used as a positive control. The doses of SOD and SOD TMC NPs were 10  $\mu\text{g}$  per ear.

After the ears were weighed, the inflamed tissues were collected, fixed by 4% formalin, dehydrated, embedded in paraffin and cut into 8  $\mu\text{m}$  sections. Finally, the sections were stained with H&E.<sup>38–40</sup> The images were observed under a conventional light microscope (Olympus IX71 inverted microscope).

### Statistical analysis

Data in this study were analyzed by the statistic package SPSS 13.0 (SPSS Inc., Chicago, IL, USA). A direct comparison between two groups was conducted by Student's non-paired *t*-test. *P*-value of  $<0.05$  was considered statistically significant. \* $P<0.05$ ; \*\* $P<0.01$ ; ns represents not significant ( $P>0.05$ ).

## Results

### Electret

Electret could be corona charged at  $\pm 500$ ,  $\pm 1,000$  and  $\pm 2,000$  V grid voltages, respectively. To evaluate the stability of electret, the surface potential of  $+2,000$  V electret was measured before and after the permeation assays. As shown in Figure 2, compared with the surface potential before the permeation assays, the surface potential did not change significantly after the permeation assays ( $P>0.05$ ), indicating that no significant charge decay happened during the permeation assays.

### Characterization of synthesized TMC

The typical peak of the *N*-trimethyl group ( $-\text{N}^+(\text{CH}_3)_3$ ) in the TMC chain was observed at 3.3 ppm (Figure 3). According to the analysis of  $^1\text{H}$  NMR, our prepared TMC possessed a DQ of 46%.

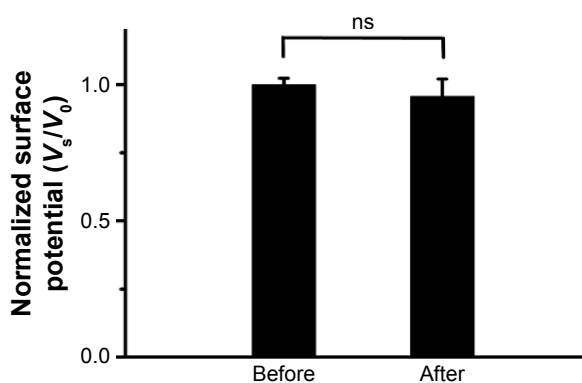


**Figure 2** Normalized surface potential ( $V_s/V_0$ ) of  $+2,000$  V electret before and after in vitro experiments.

**Notes:** Before: the normalized surface potential before in vitro experiments; After: the normalized surface potential after in vitro experiments. Data are expressed as mean  $\pm$  SD ( $n=6$ ).

**Abbreviations:** SD, standard deviation; ns, not significant.

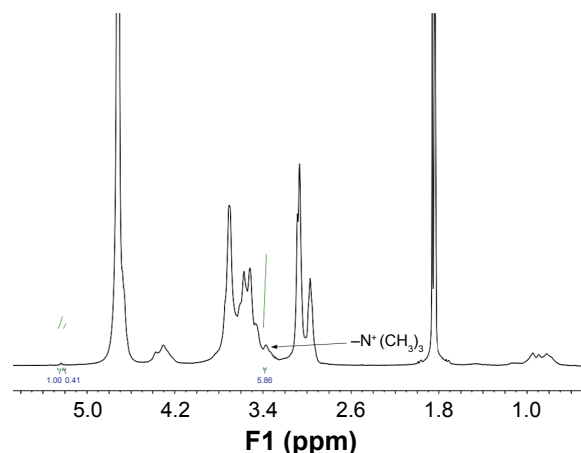


**Figure 3** The  $^1\text{H}$  NMR spectra of synthesized TMC.

**Note:** The typical peak of the *N*-trimethyl group ( $-\text{N}^+(\text{CH}_3)_3$ ) in the TMC chain was observed at 3.3 ppm (indicated by a black arrow).

**Abbreviations:** TMC, *N*-trimethyl chitosan;  $^1\text{H}$  NMR,  $^1\text{H}$  hydrogen nuclear magnetic resonance spectroscopy.

### Preparation and characterization of TMC NPs

As revealed by the TEM images (Figure 4), TMC NPs were well dispersed with little aggregation. Most NPs were of spherical shape. As shown in Table 1, the size of TMC NPs significantly increased, accompanied with the increase of pH value from 5 to 6. In contrast, with the decrease of the TMC concentration and increase of the TMC/TPP ratio, the size of TMC NPs gradually decreased. However, the zeta potential did not change significantly (26.4–28.9 mV), accompanied with the change of pH values, TMC concentrations and TMC/TPP ratios, suggesting that the above-mentioned parameters had weak effects on the zeta potential of TMC NPs. Taken together, the optimal FITC-BSA TMC NPs that had the appropriate size (150 nm) with a polydispersity index (PDI) of 0.104 were prepared at a pH value of 4.6 (acetate buffer) and a TMC/TPP ratio of 10:1, whereas the optimal SOD TMC NPs that had the appropriate size (138 nm) with a PDI of 0.117 were prepared at a pH value of 5.0 (acetate buffer) and a TMC/TPP ratio of 12:1. For the optimal FITC-BSA TMC NPs and SOD TMC NPs, the drug EE of FITC-BSA and SOD was 25% and 36%, respectively.

### In vitro skin permeation study assays

As shown in Figure 5A, the skin permeation rate of FITC-BSA TMC NPs significantly increased compared with FITC-BSA at different time points ( $P<0.01$ ). Notably,  $+2,000$  V electret further enhanced the skin permeation of FITC-BSA TMC NPs but not FITC-BSA at 12, 18 and 24 h ( $P<0.05$ ). At 24 h, the skin permeation rate of FITC-BSA TMC NPs combined with  $+2,000$  V electret was 0.12-fold higher than

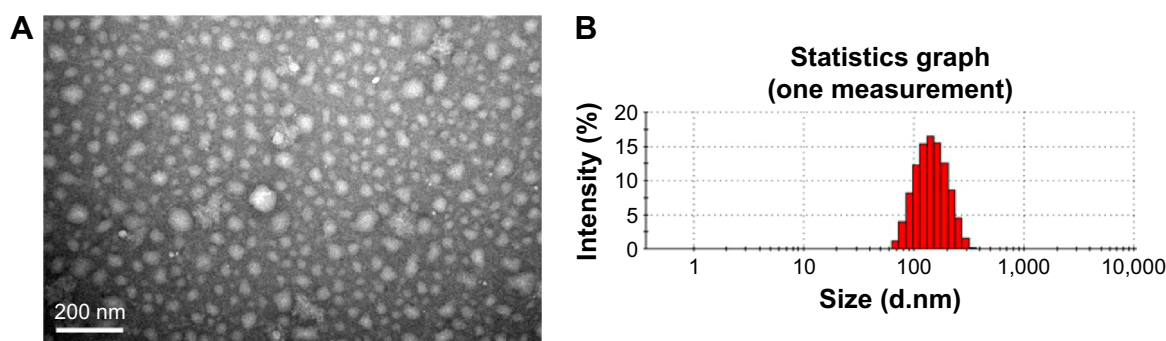


**Figure 4** The (A) shows the TEM image of TMC NPs, and (B) shows the hydrodynamic size distribution of TMC NPs in aqueous solution.

**Note:** Bar represents 200 nm.

**Abbreviations:** TEM, transmission electron microscopy; TMC, N-trimethyl chitosan; NPs, nanoparticles.

that of FITC-BSA TMC NPs ( $P < 0.05$ ). Similar results were obtained in SOD TMC NPs (Figure 5B). The skin permeation rate of SOD TMC NPs significantly increased compared with SOD at different time points ( $P < 0.01$ ). The +2,000 V electret further enhanced the skin permeation of SOD TMC NPs but not SOD at 18 and 24 h ( $P < 0.05$ ).

Figure 6 shows the skin permeation at 24 h for different skin layers (SC, epidermis and dermis). As shown in Figure 6A, the skin permeation of FITC-BSA TMC NPs significantly increased by 1.65-fold compared with FITC-BSA in the SC ( $P < 0.01$ ), and the skin permeation of FITC-BSA TMC NPs combined with +2,000 V electret was 0.33-fold higher than that of FITC-BSA TMC NPs ( $P < 0.05$ ). Similarly, in the epidermis and dermis, the skin permeation of FITC-BSA TMC NPs significantly increased by 2.45-fold compared with FITC-BSA ( $P < 0.01$ ), and the skin permeation of FITC-BSA TMC NPs combined with +2,000 V electret was 0.13-fold higher than that of FITC-BSA TMC NPs ( $P < 0.05$ ).

Similar results were obtained in SOD TMC NPs (Figure 6B). In the SC, the skin permeation of SOD TMC NPs significantly increased by 0.92-fold compared with SOD ( $P < 0.01$ ), and the skin permeation of SOD TMC

NPs combined with +2,000 V electret was 0.37-fold higher than that of SOD TMC NPs ( $P < 0.05$ ). In the epidermis and dermis, the skin permeation of SOD TMC NPs significantly increased by 4.58-fold compared with SOD ( $P < 0.01$ ), and the skin permeation of SOD TMC NPs combined with +2,000 V electret was significantly higher than that of SOD TMC NPs ( $P < 0.05$ ).

The effects of the surface voltage and the sign of the corona voltage of the electret on transdermal delivery of FITC-BSA in FITC-BSA TMC NPs are shown in Figure 7. In the groups receiving positive electret, both the +1,000 and +2,000 V electret groups showed better promoting effects on enhancing the transdermal delivery of FITC-BSA than the +500 V electret group ( $P < 0.05$ ) at 12 and 24 h, whereas the difference of the promoting effects between the +1,000 and +2,000 V electret groups was not significant ( $P > 0.05$ ). However, accompanied with increased surface voltage of negatively charged electret, the promoting effects of electret gradually decreased at 24 h. All negative electrets (-500, -1,000 and -2,000 V) showed weaker promoting effects than +2,000 V electret both at 12 and 24 h. Thus, +2,000 V electret was chosen as the optimal electret in promoting the transdermal delivery of FITC-BSA in FITC-BSA TMC NPs.

**Table 1** The influence of TMC concentration and the weight ratio of TMC/TPP on the mean particle size (nm) of TMC NPs at a range of pH values

TMC/TPP (w/w)	pH =4.6			pH =5.0			pH =5.5		
	TMC concentration (mg/mL)			TMC concentration (mg/mL)			TMC concentration (mg/mL)		
	5	10	15	5	10	15	5	10	15
6:1	139±7	181±5	273±5	202±6	236±5	297±7	242±5	282±4	423±8
10:1	108±4	140±5	207±6	159±4	172±6	224±6	216±6	236±6	360±7
12:1	105±4	135±3	189±4	127±4	138±6	186±6	187±8	196±6	342±5
15:1	104±3	127±4	180±5	126±5	133±3	176±5	172±5	190±5	336±6

**Note:** Data are expressed as mean ± SD (n=3).

**Abbreviations:** TMC, N-trimethyl chitosan; TPP, tripolyphosphate; NPs, nanoparticles; SD, standard deviation.

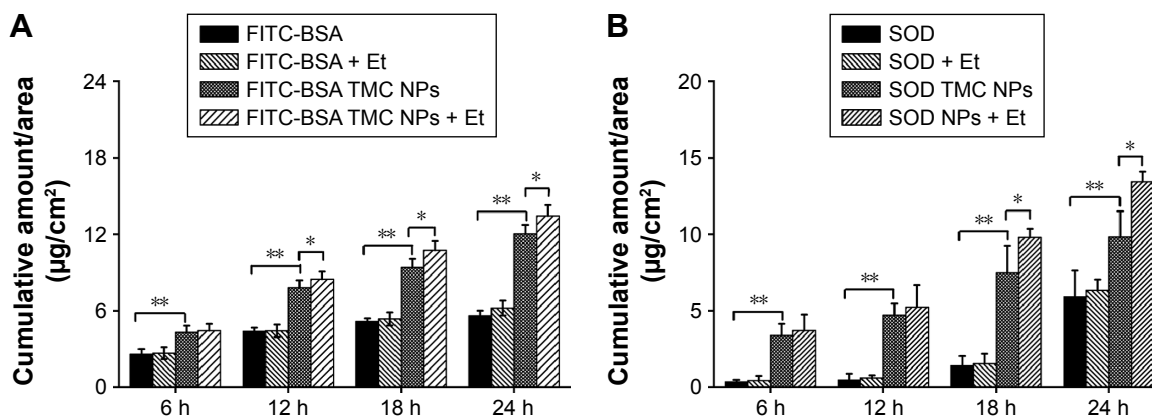


**Figure 5** In vitro skin permeation assays of (A) FITC-BSA and (B) SOD across the rat skin at different time points up to 24 h.

**Notes:** The skin permeation amount expressed as cumulative amount ( $\mu\text{g}/\text{cm}^2$ ) of FITC-BSA or SOD in the skin was analyzed by spectrofluorophotometry or ELISA, respectively. "+ Et" means "combined with +2,000 V electret". Data are expressed as mean  $\pm$  SD ( $n=6$ ). \* $P<0.05$ ; \*\* $P<0.01$ .

**Abbreviations:** FITC, fluorescein isothiocyanate; BSA, bovine serum albumin; SOD, superoxide dismutase; ELISA, enzyme-linked immunosorbent assay; Et, electret; SD, standard deviation; TMC, *N*-trimethyl chitosan; NPs, nanoparticles; h, hours.

In the receptor compartment and different skin layers, quantitative analysis of the amount of TMC NPs was performed, where FITC-TMC NPs were detected in the receptor compartment, as shown in Figure 8. Driven by the electret, the skin permeation of FITC-TMC NPs was significantly higher than that of FITC-TMC NPs at 18 and 24 h ( $P<0.05$ ). In the SC, the amount of FITC-TMC was significantly higher than that of both FITC-TMC NPs and FITC-TMC NPs combined with electret. On the contrary, a lesser amount of FITC-TMC

was detected in the epidermis and dermis compared to the other two groups. Additionally, a larger amount of FITC-TMC NPs was detected when combined with electrets, compared with FITC-TMC NPs in the epidermis and dermis ( $P<0.05$ ).

### Confocal microscopic studies

To directly examine the penetration and distribution of the protein drugs and TMC NPs, the skin sections were obtained. As shown in Figure 9A, the green fluorescence intensity

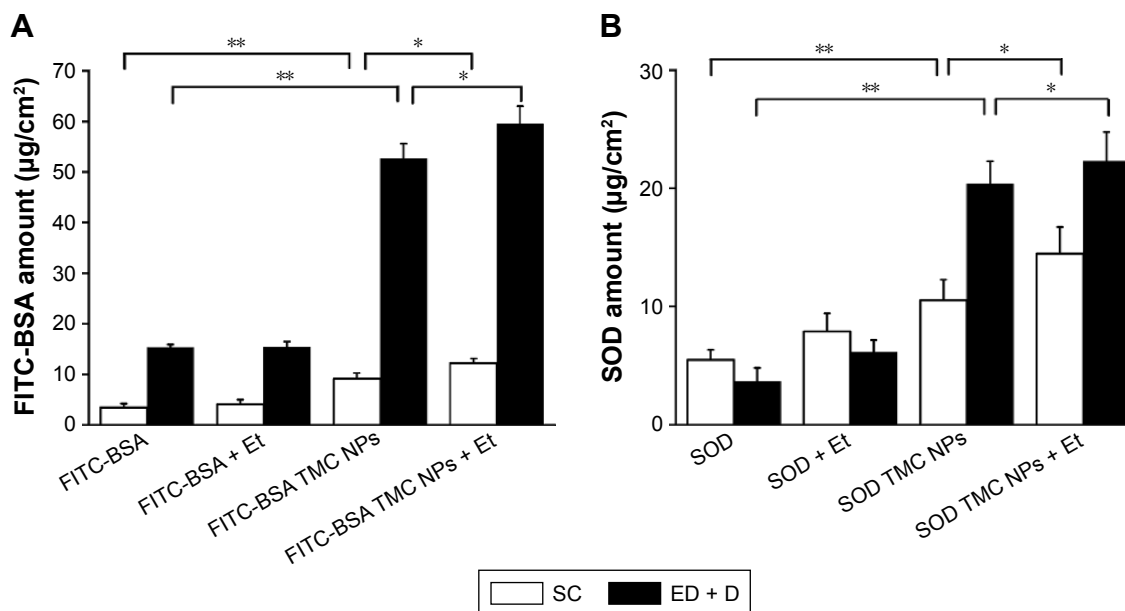


**Figure 6** The quantitative analysis of (A) FITC-BSA and (B) SOD in different layers of the skin (the SC or the epidermis and dermis) after 24 h in the in vitro skin permeation assays.

**Notes:** The skin permeation amount expressed as cumulative amount ( $\mu\text{g}/\text{cm}^2$ ) of FITC-BSA or SOD in the skin was analyzed by spectrofluorophotometry or ELISA, respectively. "+ Et" means "combined with +2,000 V electret". Data are expressed as mean  $\pm$  SD ( $n=6$ ). \* $P<0.05$ ; \*\* $P<0.01$ .

**Abbreviations:** FITC, fluorescein isothiocyanate; BSA, bovine serum albumin; SOD, superoxide dismutase; SC, stratum corneum; ELISA, enzyme-linked immunosorbent assay; Et, electret; SD, standard deviation; ED, epidermis; D, dermis; TMC, *N*-trimethyl chitosan; NPs, nanoparticles.

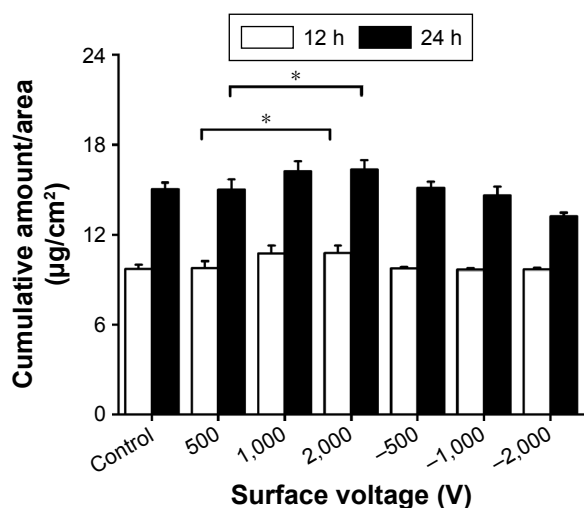


**Figure 7** The effect of surface voltage and the sign of the corona voltage of electrets in the in vitro skin permeation assays of FITC-BSA TMC NPs at 12 or 24 h.

**Notes:** The skin permeation amount expressed as cumulative amount (µg/cm<sup>2</sup>) of FITC-BSA in the skin was analyzed by spectrofluorophotometry. Data are expressed as mean ± SD (n=6). \*P<0.05.

**Abbreviations:** FITC, fluorescein isothiocyanate; BSA, bovine serum albumin; TMC, N-trimethyl chitosan; NPs, nanoparticles; SD, standard deviation.

of the skin treated with FITC-BSA TMC NPs combined with +2,000 V electret was the strongest, whereas much lower green fluorescence intensity was seen in the skin treated with FITC-BSA, FITC-BSA combined with +2,000 V electret and FITC-BSA TMC NPs. Similar results were obtained in the penetration of FITC-TMC NPs (Figure 9B). FITC-TMC NPs combined with +2,000 V electrets showed the strongest intensity of green fluorescence. As expected, negligible green fluorescence was found in untreated skin. Using the

NIH ImageJ software, a quantitative analysis of the green fluorescence also demonstrated that the green fluorescence intensity of the skin treated with FITC-BSA TMC NPs combined with +2,000 V electret was the strongest (Table 2).

### Histological examinations

The morphological change of the skin treated by +2,000 V electret was also investigated (Figure 10). As expected, untreated skin exhibited a normal structure, with orderly arranged squamous cells and intact SC. Surprisingly, after treatment with +2,000 V electret, the SC became slightly looser and thinner after 4 h. After 8 or 12 h, the SC became significantly looser and thinner, and some lacunas could be even found in the SC.

### Anti-inflammatory assays in mice

The increment of the weight of the ear in mice treated by xylene was used to measure the anti-inflammatory effects of different formulations (Figure 11A). After treatment with xylene, the mean ear weight of the control mice was increased from 24 to 52 mg. After topical application of SOD or SOD combined with electret, the ear edema degree was decreased from 28 to 25 mg, while this reduction was not significant (P>0.05). Interestingly, the ear edema degree was decreased from 28 to 20 mg after treatment with SOD TMC NPs (P<0.05). The ear edema degree was further reduced by SOD TMC NPs combined with +2,000 V electret, reaching a low value of 17 mg, which is significantly lower than SOD TMC NPs (P<0.05). In contrast, +2,000 V electret did not enhance

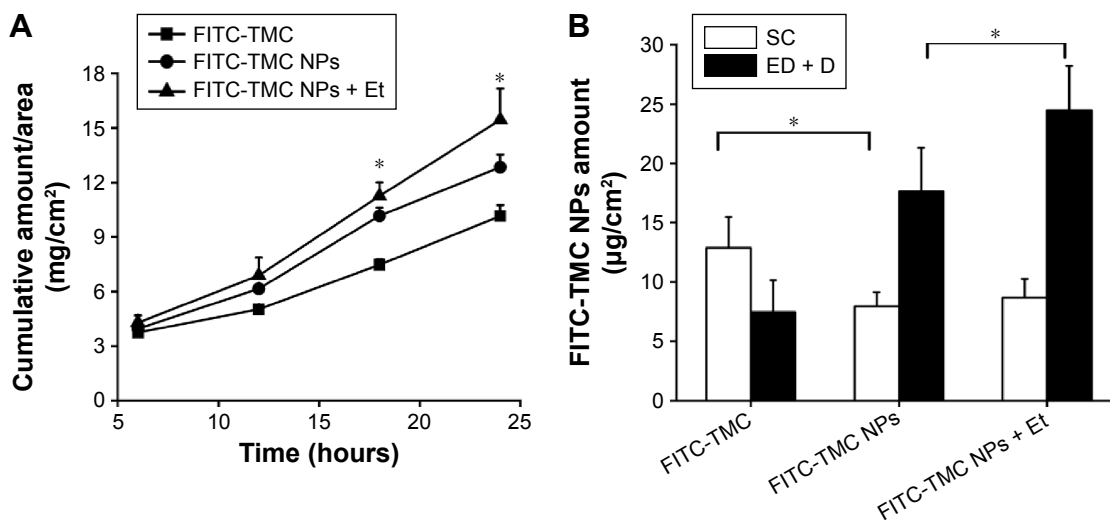


**Figure 8** Quantitative analysis of FITC-TMC NPs in the (A) receptor compartment (\*P<0.05; FITC-TMC NPs vs FITC-TMC NPs + Et) and (B) different layers of the skin (the SC or the epidermis and dermis) after 24 h in the in vitro skin permeation assays.

**Notes:** “+ Et” means “combined with +2,000 V electret”. Data are expressed as mean ± SD (n=6).

**Abbreviations:** FITC, fluorescein isothiocyanate; TMC, N-trimethyl chitosan; NPs, nanoparticles; Et, electret; SC, stratum corneum; SD, standard deviation; ED, epidermis; D, dermis.



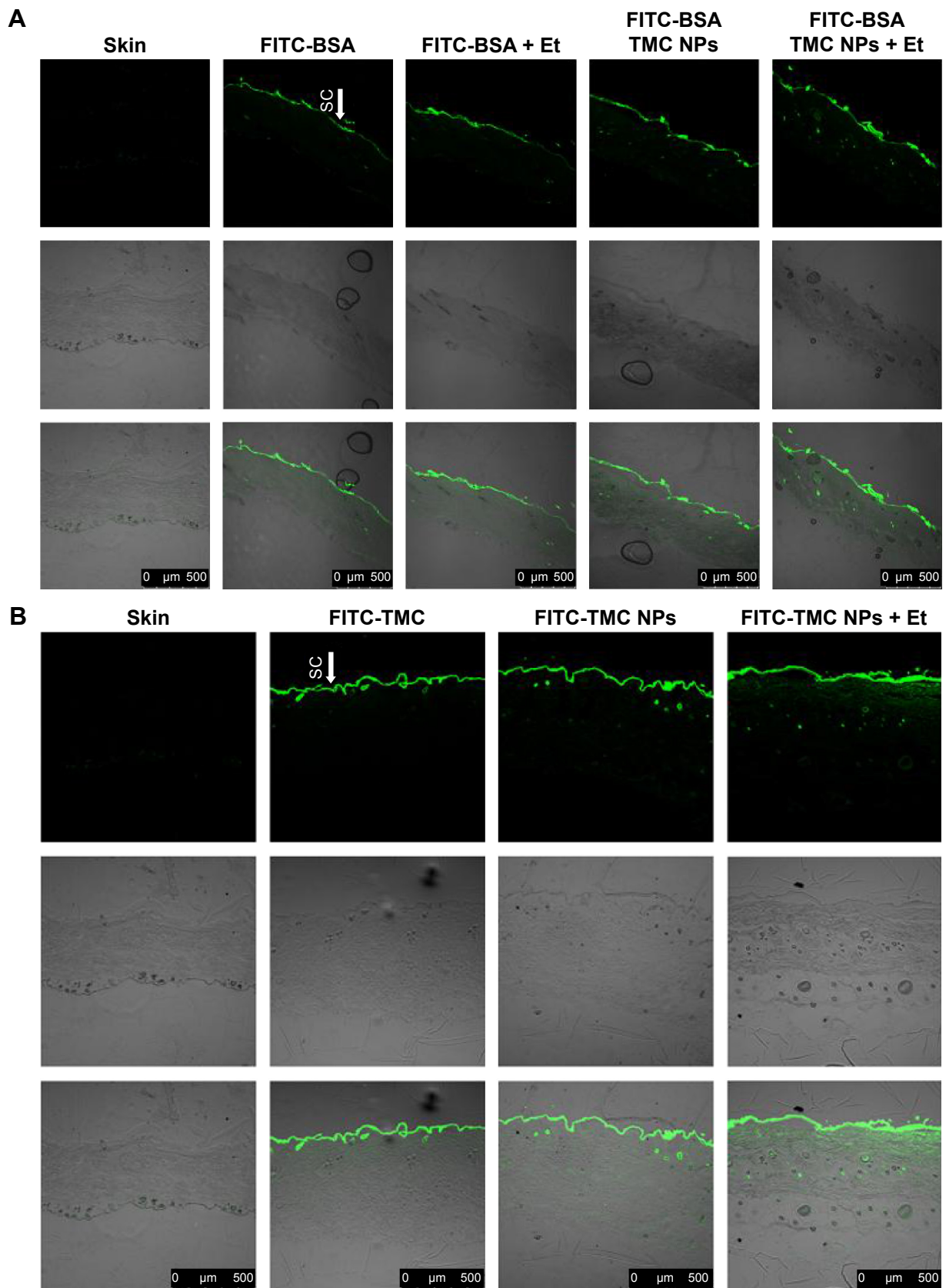


**Figure 9** Confocal microscopic studies.

**Notes:** The representative fluorescent images show the permeation and distribution of (A) FITC-BSA and (B) FITC-TMC NPs in the in vitro skin permeation assays at 24 h. Bars represent 500  $\mu$ m.

**Abbreviations:** FITC, fluorescein isothiocyanate; BSA, bovine serum albumin; TMC, N-trimethyl chitosan; NPs, nanoparticles; Et, electret; SC, stratum corneum.

**Table 2** The quantitative analysis of the relative fluorescence intensity of the skin after in vitro skin penetration assays analyzed by using the NIH ImageJ software

Relative intensity (au)		
Groups	FITC-BSA	FITC-TMC NPs
Only skin	1.1±0.1	0.8±0.1
Proteins	3.1±0.1	–
Proteins + Et	3.3±0.1	–
TMC	–	2.8±0.2
TMC NPs	4.8±0.2	7.3±0.2
TMC NPs + Et	6.7±0.2	11.4±0.1

**Note:** The data represented the mean ± standard deviation with three independent experiment.

**Abbreviations:** FITC, fluorescein isothiocyanate; BSA, bovine serum albumin; TMC, *N*-trimethyl chitosan; NPs, nanoparticles; Et, electret.

the anti-inflammation effect of SOD ( $P>0.05$ ). As expected, indomethacin exhibited excellent anti-inflammatory activity. These results are also demonstrated in Figure 11B. After treatment with SOD TMC NPs or SOD TMC NPs combined with electret, the inflammatory symptoms were greatly improved compared to the control group. Further, SOD TMC

NPs combined with electret showed better anti-inflammatory effect than SOD TMC NPs. The positive drug indomethacin showed the best anti-inflammatory effect, as expected.

## Discussion

Transdermal delivery of protein drugs is very attractive. However, the permeability of skin to protein drugs is extremely low because of the formidable barrier function of the SC. Currently, a variety of NPs, physical methods and penetration enhancers have been used to enhance the transdermal delivery of protein drugs. Our previous studies showed that electret could effectively enhance the transdermal delivery of several drugs of low molecular weight, whereas protein drugs of high molecular weight have never been investigated. Although TMC has been studied extensively and has been reported to be efficient in promoting transdermal penetration, the application of TMC NPs as a transdermal delivery system for proteins has not been reported. In this study, we have developed TMC NPs as nanocarriers for protein drugs and investigated whether electret could enhance the

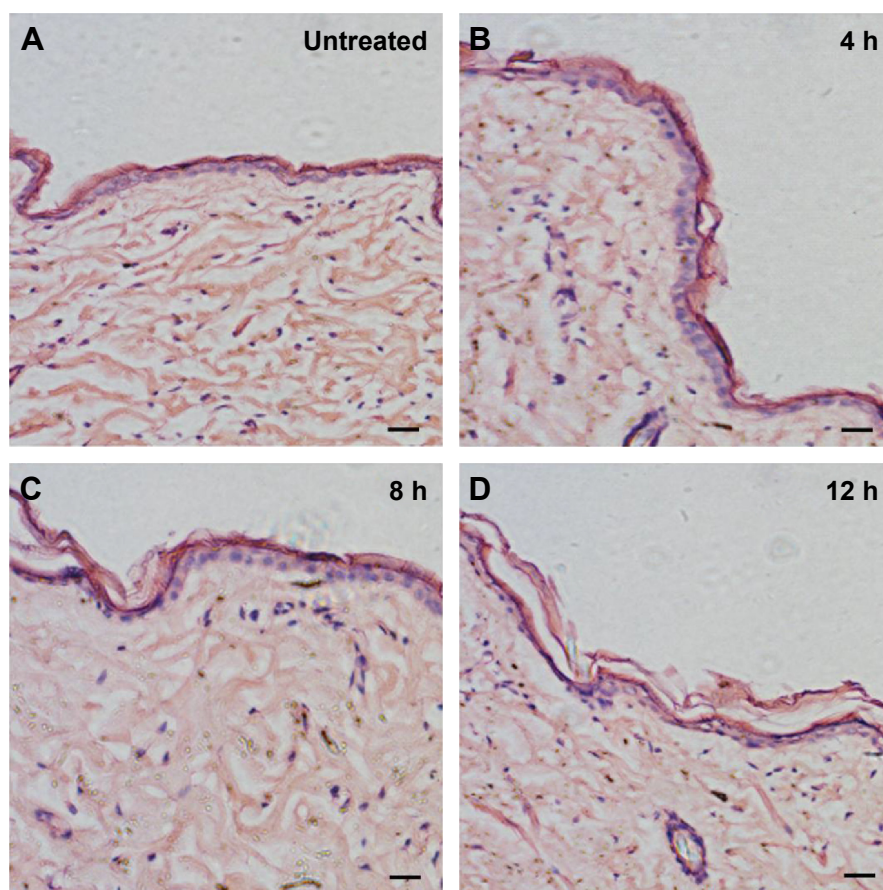


**Figure 10** The histological examinations of the skin when treated by +2,000 V electret for different periods of time (untreated, 4, 8 and 12 h).

**Notes:** The skin was stained by H&E staining. Bars represent 50  $\mu$ m.

**Abbreviations:** H&E, hematoxylin and eosin; h, hours.

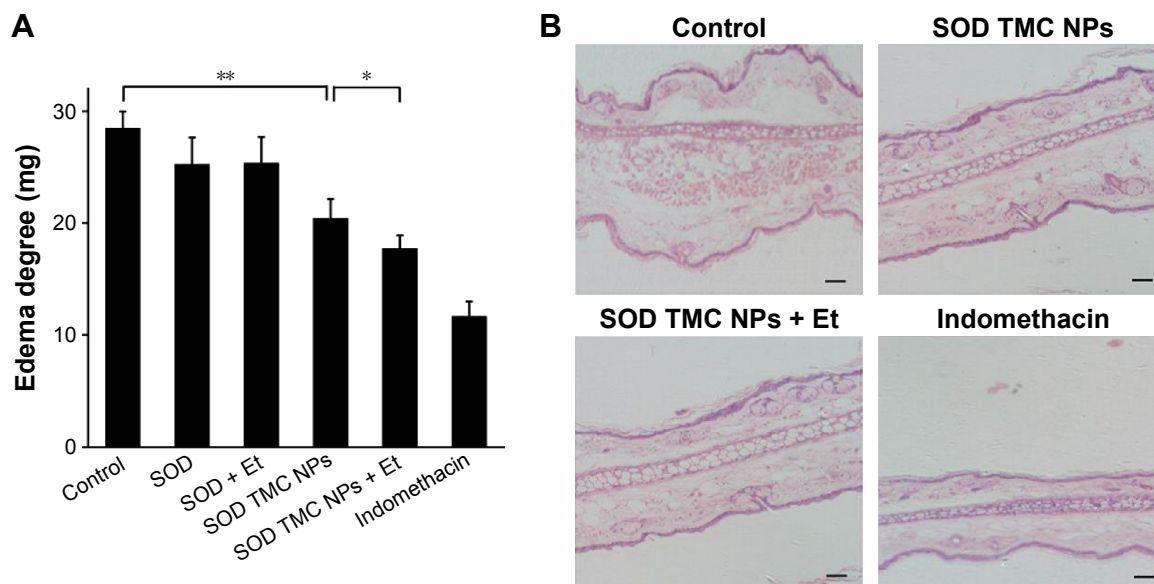


**Figure 11** Anti-inflammatory assays in mice.

**Notes:** (A) The effect of different formulations on xylene-induced edema in the ear of BALB/c mice. Six hours after transdermal delivery of different drugs (indomethacin was used as a positive control), the edema in the ear of mice was induced by xylene. Half an hour after xylene administration, the edema degree of the ear in mice was calculated by subtracting the weight of the left ear from the weight of the right ear. Data are expressed as mean  $\pm$  SD (n=6). (B) The H&E staining of the ear in mice in (A). Bars represent 50  $\mu$ m. \* $P$ <0.05; \*\* $P$ <0.01.

**Abbreviations:** SD, standard deviation; H&E, hematoxylin and eosin; SOD, superoxide dismutase; TMC, *N*-trimethyl chitosan; NPs, nanoparticles.

transdermal delivery of protein drugs. The results showed that the skin permeation of TMC NPs loaded with protein drugs was significantly enhanced by electret. Furthermore, SOD-loaded TMC NPs combined with electret exhibited the best anti-inflammatory effect in mice treated with xylene. We speculated that the promoting effect of electret in enhancing transdermal delivery of TMC NPs is attributed to the change in the structure of the SC by treatment with electret.

Our TMC NPs combined with electrets is a non-toxic, stable, flexible and convenient system, which provides a novel platform for transdermal delivery of protein drugs. First, chitosan has many excellent properties, such as non-toxicity, biodegradability and bioadhesion.<sup>26</sup> Furthermore, its promoting effect in enhancing transdermal delivery of drugs has also been well defined in several previous studies.<sup>27,32</sup> TMC NPs loaded with protein drugs were prepared by a simple ionic crosslinking method. This method is mild and could retain the activity of protein drugs. Furthermore, unlike previous methods for preparing chitosan-based transdermal NPs,<sup>1,2</sup> this method did not introduce any extra organic solvents, which may be harmful for human health. TMC NPs also exhibited superior stability, and their size did not change significantly at 4°C in 30 days. Second, electret is an excellent charge container. We demonstrated that, even after the transdermal experiment, all electrets could still hold 95% of their initial charge, suggesting that the PP

electret used in this study had good charge storage stability. This good charge stability guarantees that the electrostatic field produced by the electret could persistently promote the transdermal delivery of protein drugs. Third, the application of PP electret is very flexible, and we only need to place the electret above the surface of the drugs for a period of time, after administration of the drugs.

Our studies showed that skin permeation of TMC NPs significantly increased compared with free protein drugs. It is very meaningful that TMC NPs can promote the transdermal delivery of protein drugs to a much greater extent in the epidermis and dermis than in the SC, indicating that TMC NPs could deeply penetrate into the skin. The superior accumulation of TMC NPs in the epidermis and dermis than in the SC would greatly contribute to local treatment of skin diseases. Strikingly, electret further enhanced the skin permeation of TMC NPs but not free protein drugs, and TMC NPs achieved the most effective transdermal delivery of protein drugs. We speculated that the mechanisms, by which TMC NPs combined with electret achieved the most effective transdermal delivery of protein drugs, are as follows. First, the powerful electrostatic repulsive force between TMC NPs and electret makes TMC NPs quickly penetrate through the skin. Second, TMC NPs may loosen the compact structure of keratin in the SC, widen the tight junctions in the skin and/or penetrate the skin through hair follicles. Third, electret can

change the structure of the skin and make the skin thinner and looser, resulting in feasible transport of TMC NPs through the skin. Our histological examinations demonstrated that electret could affect the structure of SC and make the SC thinner and looser, resulting in decreased transdermal permeation resistance and enhanced transdermal drug delivery. In contrast, electret has minimal effects on free protein drugs, due to the large molecular weight of protein drugs<sup>23</sup> and the lack of enough electrostatic repulsive forces.

To elucidate the mechanism of skin permeation of TMC NPs, the penetration and distribution of FITC-TMC NPs were also investigated. The results showed that FITC-TMC NPs were detected in the receptor compartment, and a larger amount of TMC NPs was detected in the epidermis and dermis layers than in the SC layers. Thus, we speculated that enhanced protein delivery by TMC NPs was due to the transport of the TMC NPs themselves. Similar results were obtained in the penetration of TMC NPs themselves (green fluorescence of FITC) and FITC-BSA (Figure 9), which was in good accordance with quantitative analysis discussed earlier.

Furthermore, the surface voltage and the sign of the corona voltage of the electret were optimized in our study. Our results showed that the skin permeation of protein drugs increased, accompanied with the increase of surface voltage of positively charged electret. In contrast, the skin permeation gradually decreased, accompanied with an increase of surface voltage of negatively charged electret. We speculated that higher positive surface voltage of electret could offer stronger electrostatic repulsive force to drive more NPs penetrate into deeper skin layers. In contrast, negative surface voltage of electret could offer electrostatic attractive force, which plays a negative role in promoting the transdermal delivery of protein drugs. Thus, +2,000 V electret was chosen as the optimal electret in promoting the transdermal delivery of TMC NPs.

Finally, we used SOD as a model drug to measure the anti-inflammatory effect of SOD TMC NPs. As expected, SOD TMC NPs combined with electret showed the most excellent anti-inflammatory activity, suggesting that TMC NPs combined with electret represent a novel platform for transdermal delivery of protein drugs.

## Conclusion

Collectively, the novel delivery system, TMC NPs combined with electret, has great potential in transdermal delivery of protein drugs. Our in vitro permeation studies and a confocal laser scanning microscopy demonstrated a decent transdermal delivery efficiency of protein drugs using TMC NPs in

the presence of electrets. Notably, SOD-loaded TMC NPs combined with electret exhibited the best inhibitory effect on the edema of the mouse ear. Three proposed mechanisms may contribute to the superior transdermal delivery of TMC NPs combined with electret: the powerful electrostatic repulsive force between TMC NPs and electret; TMC NPs may loosen the compact structure of keratin in SC and widen the tight junctions in the skin; electret can change the structure of the skin and make the skin thinner and looser. In summary, TMC NPs combined with electret represent a novel platform for transdermal delivery of protein drugs.

## Acknowledgments

We thank Professor Jian Jiang (the Second Military Medical University, Shanghai, China) for his technical help in preparing electret and for useful suggestions in preparing this manuscript. This work was financially supported by the National Natural Science Foundation of China (no 81000689).

## Disclosure

The authors report no conflicts of interest in this work.

## References

- Choi WI, Lee JH, Kim JY, Kim JC, Kim YH, Tae G. Efficient skin permeation of soluble proteins via flexible and functional nano-carrier. *J Contr Rel.* 2012;157(2):272–278.
- Shah PP, Desai PR, Patel AR, Singh MS. Skin permeation nanogel for the cutaneous co-delivery of two anti-inflammatory drugs. *Biomaterials.* 2012;33(5):1607–1617.
- Praustz MR, Langer R. Transdermal drug delivery. *Nat Biotechnol.* 2008;26(11):1261–1268.
- Karande P, Jain A, Mitragotri S. Discovery of transdermal penetration enhancers by high-throughput screening. *Nat Biotechnol.* 2004;22(2):192–197.
- Li Z, Hao TN, Ding PT, et al. Effect of pH, vehicles and chemical enhancers on the skin permeation of loratadine. *Lat Am J Pharm.* 2011;30(3):534–539.
- Kalia YN, Naik A, Garrison J, Guy RH. Iontophoretic drug delivery. *Adv Drug Deliv Rev.* 2004;56(5):619–658.
- Yan G, Peck KD, Zhu H, Higuchi WI, Li SK. Effects of electrophoresis and electroosmosis during altering current iontophoresis across human epidermal membrane. *J Pharm Sci.* 2005;94(3):547–558.
- Prausnitz MR, Bose VG, Langer R, Weaver JC. Electroporation of mammalian skin: a mechanism to enhance transdermal drug delivery. *Proc Natl Acad Sci U S A.* 1993;90(22):10504–10508.
- Sullivan SP, Murthy N, Prausnitz MR. Minimally invasive protein delivery with rapidly dissolving polymer microneedles. *Adv Mater.* 2008;20(5):933–938.
- Wendorf JR, Ghartey-Tagoe EB, Williams SC, Enioutina E, Singh P, Cleary GW. Transdermal delivery of macromolecules using solid-state biodegradable microstructures. *Pharm Res.* 2011;28(28):22–30.
- Mitragotri S, Blankshtein D, Langer R. Ultrasound-mediated transdermal protein delivery. *Science.* 1995;269(5225):850–853.
- Tachibana K. Transdermal delivery of insulin to alloxan-diabetic rabbits by ultrasound exposure. *Pharm Res.* 1992;9(7):952–954.
- Lee WR, Shen SC, Wang KH, Hu CH, Fang JY. The effect of laser treatment on skin to enhance and control transdermal delivery of 5-fluorouracil. *J Pharm Sci.* 2002;91(7):1613–1626.

14. Hurkmans JF, Boddé HE, Van Driel LM, Van Doorne H, Junginger HE. Skin irritation caused by transdermal drug delivery systems during long-term (5 days) application. *Br J Dermatol*. 1985;112(4):461–467.
15. Barry BW. Breaching the skin's barrier to drugs. *Nat Biotechnol*. 2004; 22(2):165–167.
16. Sessler GM. *Electrets*. New York: Springer-Verlag; 1987.
17. Jiang J, Liang YY, Dong FJ, Liu HY, Tu Y, Cui LL. Study of electret effect of rat skin by thermally stimulated discharge analysis. *J Electrostat*. 2012;70(3):258–263.
18. Cui LL, Liang YY, Dong FJ, et al. Structure of rat skin after application of electrets characterized by DSC. *J Phys Con Series*. 2011;301(1): 012027.
19. Cui LL, Jiang J, Zhang L, Song CR, Zhao WQ, Lin JM. Enhancing effect of electrets on transdermal drug delivery. *J Electrostat*. 2001;51(1): 153–158.
20. Cui LL, Hou XM, Jiang J, Li GD, Liang YY, Xin X. Effects of electret with chemical enhancement on transdermal delivery of meloxicam in vitro. *J Phys Con Aeries*. 2008;142:012015.
21. Kong YX, Cheng L, Xiao YH, Wang D, Jiang J, Cui LL. Enhancing effects of electret on transdermal delivery of lidocaine patches in vitro. *Acad J Second Military Med Univ*. 2009;30(5):469–472.
22. Cui LL, Liu HY, Ma L, Liang YY, Jiang J. Enhanced transdermal delivery of cyclosporine A by PP electret and ethyl oleate. *IEEE T Dielect El In*. 2012;19:1191–1194.
23. Murthy NS, Boguda VA, Payasada K. Electret enhances transdermal drug permeation. *Biol Pharm Bull*. 2008;31(1):99–102.
24. Spara B, Jain S, Tiwary AK. Effect of *Asparagus racemosus* extract on transdermal delivery of carvedilol: a mechanistic study. *AAPS PharmSciTech*. 2009;10:199–210.
25. Smith J, Wood E, Dornish M. Effect of chitosan on epithelial cell tight junctions. *Pharm Res*. 2004;21(1):43–49.
26. He W, Guo X, Xiao L, Feng M. Study on the mechanisms of chitosan and its derivatives used as transdermal penetration enhancers. *Int J Pharm*. 2009;382(1–2):234–243.
27. Hamman JH, Stander M, Kotzé AF. Effect of the degree of quaternisation of N-trimethyl chitosan chloride on absorption enhancement: in vivo evaluation in rat nasal epithelia. *Int J Pharm*. 2002;232(1–2): 235–242.
28. Jonker C, Hamman JH, Kotzé AF. Intestinal paracellular permeation enhancement with quaternised chitosan: in situ and in vitro evaluation. *Int J Pharm*. 2002;238(1–2):205–213.
29. Di Colo G, Burgalassi S, Zambito Y, Nardini I, Saettone MF. Effect of chitosan and of N-carboxymethyl chitosan on intraocular penetration of topically applied ofloxacin. *Int J Pharm*. 2004;273(1–2):37–44.
30. Sandri G, Rossi S, Bonferoni MC, et al. Buccal penetration enhancement properties of N-trimethyl chitosan: influence of quaternization degree on absorption of a high molecular weight molecule. *Int J Pharm*. 2005; 297(1–2):146–155.
31. Bal SM, Slutter B, Verheul R, Bouwstra JA, Jiskoot W. Adjuvanted, antigen loaded N-trimethyl chitosan nanoparticles for nasal and intradermal vaccination: adjuvant- and site-dependent immunogenicity in mice. *Eur J Pharm Sci*. 2012;45(4):475–481.
32. He W, Guo X, Zhang M. Transdermal permeation enhancement of N-trimethyl chitosan for testosterone. *Int J Pharm*. 2008;356(1–2): 82–87.
33. Hentz NG, Richardson JM, Sportsman JR, Daijo J, Sittampalam GS. Synthesis and characterization of insulin-fluorescein derivatives for bioanalytical applications. *Anal Chem*. 1997;69(24):4994–5000.
34. Qian F, Cui FY, Ding JY, Tang C, Yin CH. Chitosan graft copolymer nanoparticles for oral protein drug delivery: preparation and characterization. *Biomacromolecules*. 2006;7(10):2722–2727.
35. Hamman JH, Kotze AF. Effect of the type of base and number of reaction steps on the degree of quaternization and molecular weight of N-trimethyl chitosan chloride. *Drug Dev Ind Pharm*. 2001;27(5): 373–380.
36. Zhu SY, Qian F, Zhang Y, Cui T, Yin C. Synthesis and characterization of PEG modified N-trimethylaminoethylmethacrylate chitosan nanoparticles. *Eur Polym J*. 2007;43(6):2244–2253.
37. Kajimoto K, Yamamoto M, Watanabe M, et al. Noninvasive and persistent transfollicular drug delivery system using a combination of liposomes and iontophoresis. *Int J Pharm*. 2011;403(1–2):57–65.
38. Yu HL, Zhang F, Li YJ, Gong GH, Quan ZS. Anti-inflammatory and antinociceptive effects of 6-(4-chlorophenoxy)-tetrazolo[5,1-a]phthalazine in mice. *Pharmacol Rep*. 2012;64(5):1155–1165.
39. Zhang JQ, Wang HS, Wang T, et al. Anti-inflammatory activity of Yanshu spraying agent in animal models. *Exp Ther Med*. 2013;5(1): 73–76.
40. Siomes S, Marques C, Cruz ME, Martins MBF. Anti-inflammatory effects of locally applied enzyme-loaded ultradeformable vesicles on an acute cutaneous model. *J Microencapsul*. 2009;26(7):649–658.

## International Journal of Nanomedicine

### Publish your work in this journal

The International Journal of Nanomedicine is an international, peer-reviewed journal focusing on the application of nanotechnology in diagnostics, therapeutics, and drug delivery systems throughout the biomedical field. This journal is indexed on PubMed Central, MedLine, CAS, SciSearch®, Current Contents®/Clinical Medicine,

Submit your manuscript here: <http://www.dovepress.com/international-journal-of-nanomedicine-journal>

Dovepress

Journal Citation Reports/Science Edition, EMBASE, Scopus and the Elsevier Bibliographic databases. The manuscript management system is completely online and includes a very quick and fair peer-review system, which is all easy to use. Visit <http://www.dovepress.com/testimonials.php> to read real quotes from published authors.